Seismic Behavior of Floating Houses

C. S. Tsai
Department of Civil Engineering, Feng Chia University, Taichung, Taiwan

H. C. Su
Department of Water Resources Engineering and Conservation, Feng Chia University, Taichung, Taiwan

W.C. Liao
Department of Civil Engineering, Feng Chia University, Taichung, Taiwan

Y. M. Wang
Graduate Institute of Civil and Hydraulic Engineering, Feng Chia University, Taichung, Taiwan

SUMMARY:
Inhabitable land has been decreasing due to the continual rise in sea levels caused by global warming. In response to this climate change, we need to consider looking for living spaces on water surfaces as well as building earthquake-resistant structures, particularly in flood and earthquake prone areas. Presented in this paper is an experimental study on the seismic behavior of a floating house that is located in a port. Based on experimental observations, the seismic response of various types of floating houses were considerably different from those of traditional structures built on a ground surface. Experimental results from this study suggest building codes established for traditional buildings should be reconsidered for houses built on a sea surface. In addition, earthquake proof technology such as base isolation and energy absorbing systems may be considered good tools for safeguarding floating houses from earthquake damage.

Keywords: Floating house, seismic behaviour, base isolation, earthquake proof systems, structural control

1. INTRODUCTION

Base isolation technology has been recognized as a promising technique for preventing existing and new structures from earthquake damage. Among the sliding type base isolation systems developed in the past, a friction pendulum system (FPS) isolation device with a concave sliding surface and an articulated slider was proposed by Zayas et al. (1987). The FPS isolator has been proven in theory and in experiment studies to be an efficient device for reducing the seismic responses of structures (Zayas et al. 1987, Al-Hussaini et al. 1994, Tsai 1997, Jangid 2005). For enhancing the earthquake- proof efficiency and reducing the size of the FPS isolator, a multiple friction pendulum system (MFPS) with double concave surfaces and an articulated slider located between the concave surfaces was proposed by Tsai et al. (2003a, b, c, 2004, 2005, 2006). Seismic response characteristics of bridges using the MFPS isolation system with double concave surfaces have been reported by Kim and Yun (2007). In addition, several other types of the MFPS isolator, which basically represent more than one pendulum system connected in series, were invented by Tsai et al. (2002, 2008). Follow-up research conducted on the characteristics of the MFPS isolator has been published by Fenz and Constantinou (2008). The efficiency of the MFPS isolator with four concave surfaces in mitigating seismic responses of buildings has been investigated by Morgan and Mahin (2008). However, the abovementioned base isolation systems have been tested and deployed on a land without water.

In recent years, more geographical areas are sinking due to the continual rise in sea level caused by global warming, and the low-lying land has to face worsening flooding problems due to the climate change. People are forced to find more living space on water. A building called the floating house has been adopted to solve the problems (Yang 2007). However, some potential risk, such as an earthquake, might result in damage to floating houses used in earthquake prone areas. Therefore, safeguarding floating houses in flood and earthquake prone areas has become an important issue. In this study, a scaled floating house model was investigated through a series of shaking table tests. In the shaking table tests, we observed that the seismic responses of the floating house resting on the water surface were amplified on condition that the displacement was limited by cables or rods fixed at the bottom of the cistern. Based on these observations, we proposed a base isolation system by using the nature of water properties to isolate earthquake induced energy. Experimental results showed that the seismic response of the floating house was considerably reduced by the proposed isolation system.

2. SHAKING TABLE TESTS OF A SCALED FLOATING HOUSE

In order to examine the behavior of a floating house during an earthquake, a series of shaking table tests of a one-tenth scale floating house model were carried out in the Earthquake Hazard Prevention and Control Laboratory at Feng-Chia University in Taichung, Taiwan. As shown in Figures 2.1-2.3, the one-story floating house made by stainless steel had 12 cm in each horizontal direction and 30 cm in the height. Each beam and column was 1.5 mm in thickness. As shown in Figure 2.4, the Fourier Transform (FFT) of free vibration test indicated that the fundamental natural frequency of the small scale floating house model in the weak direction was 7.03 Hz. Four types of shaking table tests were performed as follows:

1. Fixed-base type (FB type): The foundation of the floating house model was fixed on the shaking table.
2. No displacement limit type (NDL type): The floating house model could float freely in the water cistern during the tests, as shown in Figure 2.5.
3. Cable-constrained type (CC type): The floating house model was constrained at a place through cables, as shown in Figures 2.6 and 2.7.
4. Displacement limit type (DL1 & DL2 type): In this type, the scaled floating house consists of the scaled steel frame and a floating board with four holes of 16 mm or 25 mm in diameter at the corners of the board, as shown in Figures 2.8 and 2.9. Each of the four holes was pierced by one metal rod that was 25 cm in length and 12 mm in diameter. The entire model, which had the total weight of 2190 g, was placed on the water surface. Therefore, the floating house had allowable displacement capacity of ± 2 mm and ± 6.5 mm, respectively.

During the tests, a circular cistern with 1.5 m in diameter and 30 cm in maximum depth, which was filled with water to simulate a harbor with a finite area and water, was placed on the shaking table, and the water depth was about 10 cm. The floating house was located at the center of the cistern at the beginning of each ground motion. To be reasonable to simulate the situation of a real structure, the Similarity Theory had applied to the shaking table tests. The scale factor used in this study was 1/10; therefore, the corresponding frequencies such as the predominant frequency of the ground motion should be multiplied by the square root of 10. The ground motions of the El Centro (1940), Kobe (1995) and Chi-Chi (TCU068 station, 1999) earthquakes were given as input excitations during the shaking table tests. The predominant frequencies of modified and original input excitations are shown in Table 2.1.

The comparisons of the absolute roof accelerations between the scaled model and the ground motion under the EW El Centro, EW Kobe, and EW Chi-Chi earthquakes are shown in Figures 2.10 to 2.21, respectively. The values listed in Table 2.2 are ratios of the peak accelerations of the scaled model to the ground motions under various cases of the floating house types and excitations. In order to examine the response frequencies of the scaled structure and the floating board, acceleration transmissibility of the roof the floating board subjected to various earthquakes are plotted in Figures 2.22 to 2.33 as a function of frequencies.

As for the NDL type, the structural responses were usually less than the peak ground accelerations (PGA), as shown in Figures 2.10 and 2.11, but in the cases of the lower predominant frequencies, such as the Chi-Chi earthquake, the structural response was higher than the PGA, as shown in Fig. 2.12. As indicated in Figures 2.22 and 2.23, the entire structure vibrates with lower frequencies, so the ground motion with higher frequency vibrations will be isolated through water. As shown in Figure 2.12, the reason for the structural response being amplified by 2.64 times of the PGA during the EW Chi-Chi earthquake is that the floating house made a contact with the boundary of the cistern at about 25 sec. In general, water is a good isolation medium between the floating house and ground to reduce the structural response of the floating house during ground shakings.

As shown in Figures 2.13-2.21, the structural responses for the cases of the CC, DL1, and DL2 types were much higher than the PGA, which were quite different from those for the NDL type. Because the displacement capacities of the floating house in the CC, DL1, and DL2 types were limited by the tensile cables or the displacement restrainers, contacts between the floating house and the displacement restrainers or sudden tensile forces in the cables produced shock waves and impact effects to amplify the structural responses during earthquakes. The results plotted in Figures 2.25 to 2.33 show that the energy contents of structural responses due to shock and impact concentrate in the region of higher frequencies.

3. CONCLUSIONS

Various types of isolation systems for a floating house have been investigated through a series of shaking table tests. Based on the results of shaking table tests, the floating house could be protected by the natural behavior of water if no displacement limit was applied in the systems during earthquakes. It implies that the seismic energy could be isolated by the water medium that produces no shear wave during earthquakes.

REFERENCES

Al-Hussaini, T. M., Zayas, V. A. and Constantinou, M. C. (1994). Seismic isolation of multi-story frame structures using spherical sliding isolation systems. Technical Report, NCEER-94-0007.

Fenz, D. M. and M. C. Constantinou, M. C. (2008). Spherical sliding isolation bearings with adaptive behavior-theory. *Earthquake Engineering and Structural Dynamics*, **37**, 168-183.

Jangid, R. S. (2005). Optimum friction pendulum system for near-fault motions. *Engineering Structures*. **7**, 349-359.

Kim, Y. S. and Yun, C. B. (2007). Seismic response characteristics of bridges using double concave friction pendulum bearings with tri-linear behavior. *Engineering Structures*, **29**, 3082-3093.

Morgan, T. A. and Mahin, S. A. (2008). The optimization of multi-stage friction pendulum isolators for loss mitigation considering a range of seismic hazard. *14th World Conference on Earthquake Engineering*, Beijing, China, Paper No. 11-0070.

Tsai, C. S. (1997). Finite element formulations for friction pendulum isolation bearings. *International Journal for Numerical Method in Engineering.* **40:** 29-49.

Tsai, C. S. (2002). Improved structures of base isolation systems. Taiwan Patent No. 207126, Publication Number 00542278, Publication Date: July 11, 2003, Application Number 091210175, Filing date: July4, 2002 (in Chinese).

Tsai, C. S., Chiang, T. C. and Chen, B. J. (2003). Finite element formulations and theoretical study for variable curvature friction pendulum system. *Engineering Structures*,.**25**, 1719-1730.

Tsai, C. S., Chiang, T. C. and Chen, B. J. (2003). Seismic behavior of MFPS isolated structure under near-fault sources and strong ground motions with long predominant periods. *2003 ASME Pressure Vessels and Piping Conference, Seismic Engineering,* Chen, J. C. (ed.), Cleveland, Ohio, U. S. A., July, 2003, 466, 73-79.

Tsai, C. S., Chiang, T. C. and Chen, B. J. (2003). Shaking table tests of a full scale steel structure isolated with MFPS. *2003 ASME Pressure Vessels and Piping Conference,* Seismic Engineering, Chen, J. C. (ed.), Cleveland, Ohio, U. S. A., July, 2003, **466**, 41-47.

Tsai, C. S., Chen, B. J., Pong, W. S. and Chiang, T. C. (2004). Interactive behavior of structures with multiple friction pendulum isolation system and unbounded foundations. *Advances in Structural Engineering, An International Journal*, **7(6)**, 539-551.

Tsai, C. S., Chiang, T. C., Chen, B. J. (2005). Experimental evaluation piecewise exact solution for predicting seismic responses of spherical sliding type isolated structures. *Earthquake Engineering and Structural Dynamics*, **34(9)**, 1027–1046.

Tsai, C. S., Chen, W. S., Chiang, T. C. and Chen, B. J. (2006). Component and shaking table tests for full-scale multiple friction pendulum system. *Earthquake Engineering and Structural Dynamics*, **35(11)**, 1653–1675.

Tsai, C. S., Lu, P. C., Chen, W. S., Chiang, T. C., Yang C. T. and Lin, Y. C. (2008). Finite element formulation and shaking table tests of direction-optimized friction pendulum system. *Engineering Structures*, **30**, 2321-2329.

Yang, Patrick Yau Siaw. (2007). Development of Integrated Floating House - Conceptual Model for Flood Prone Area in Malaysia: Noah Project. Department of Civil Engineering, Universiti Teknologi Malaysia.
Zayas, V. A., Low, S. S. and Mahin, S. A. (1987). The FPS Earthquake Resisting System Report. EERC Technical Report, UBC/EERC-87/01.

Table 2.1. Comparisons of predominant frequencies between original and compressed input excitations

	Original	Compressed
El Centro (EW)	1.47 Hz	4.65 Hz
El Centro (NS)	1.75 Hz	5.54 Hz
Kobe (NS)	1.44 Hz	4.55 Hz
Kobe (EW)	1.38 Hz	4.35 Hz
Chi-Chi (EW)	0.38 Hz	1.19 Hz
Chi-Chi (NS)	0.11 Hz	0.35 Hz

Table 2.2. ratios of peak roof accelerations at top of the model to Peak Ground Accelerations

	FB type	NDL type	CC type	DL1 type (±2mm)	DL2 type (±6.5mm)
El Centro (EW)	3.19	0.36	3.58	3.34	4.03
El Centro (NS)	4.11	0.83	3.27	2.98	5.66
Kobe (NS)	2.63	0.96	3.07	4.07	6.08
Kobe (EW)	2.10	0.73	4.28	3.42	5.53
Chi-Chi (EW)	1.77	2.64*	6.29	5.11	6.64
Chi-Chi (NS)	1.44	1.04	7.48	3.42	4.81
*: contact made with the boundary of the cistern					

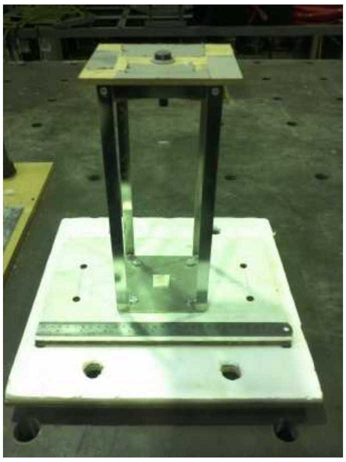

Figure 2.1. Front view of The scaled floating house model

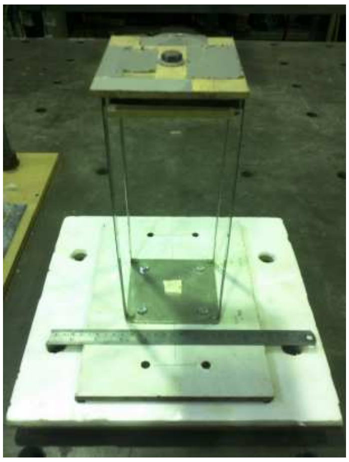

Figure 2.2. Side view of The scaled floating house model

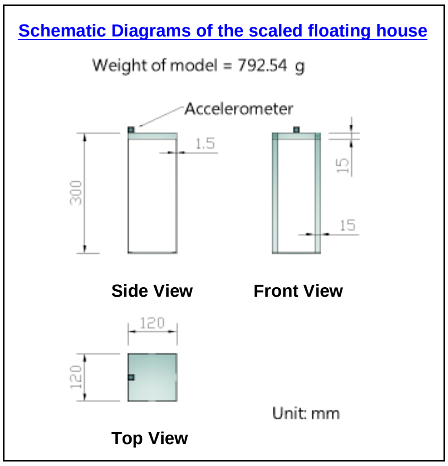

Figure 2.3. Schematic diagrams of The scaled floating house from various views

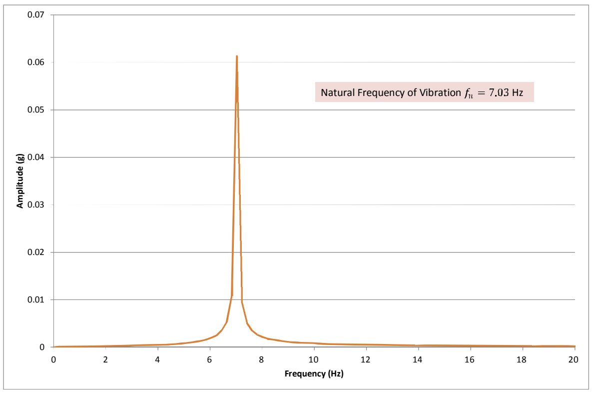

Figure 2.4. Fourier Transform of the roof acceleration under Free Vibrations

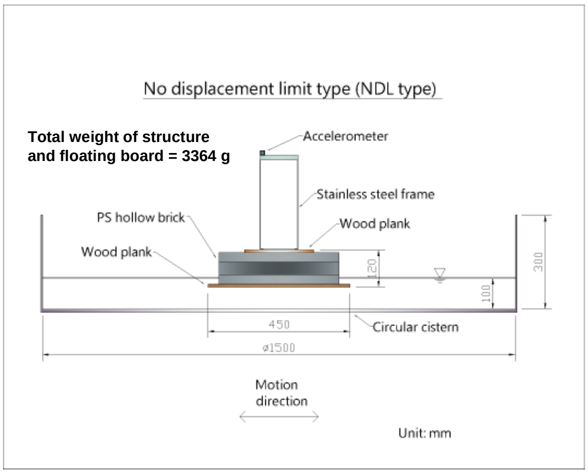

Figure 2.5. Schematic diagram of the NDL type arragement (side view)

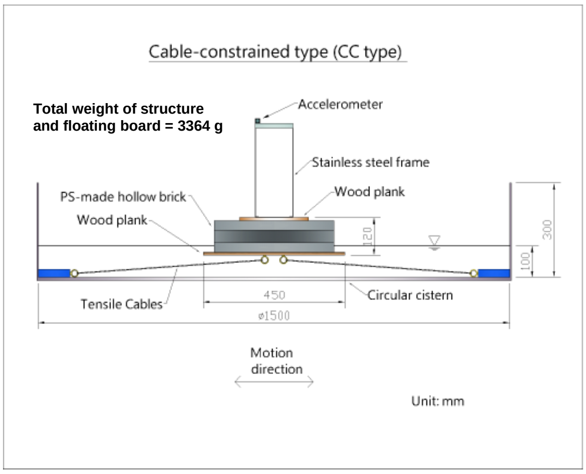

Figure 2.6. Schematic diagram of the CC type Arragement (side View)

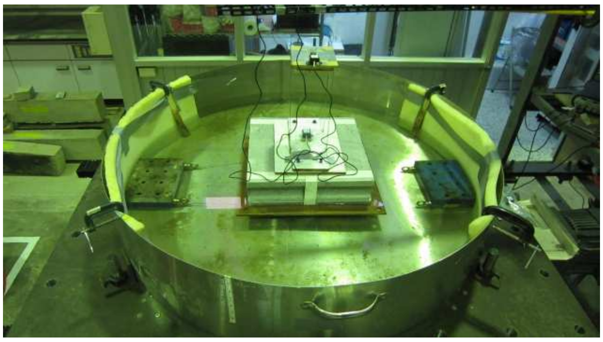

Figure 2.7. floating house model Resting on water surface of a cistern (CC type)

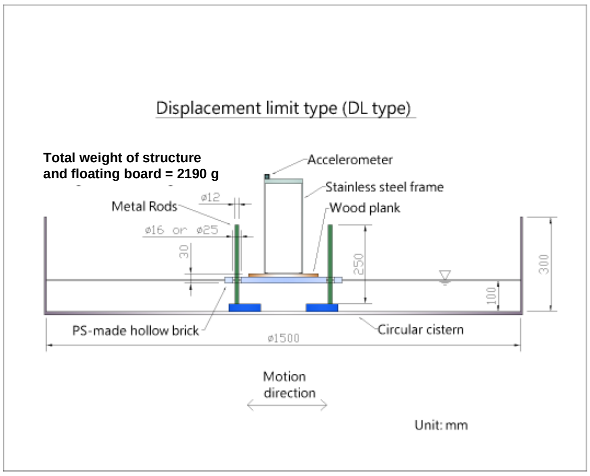

Figure 2.8. Schematic diagram of the DL type Arragement (side view)

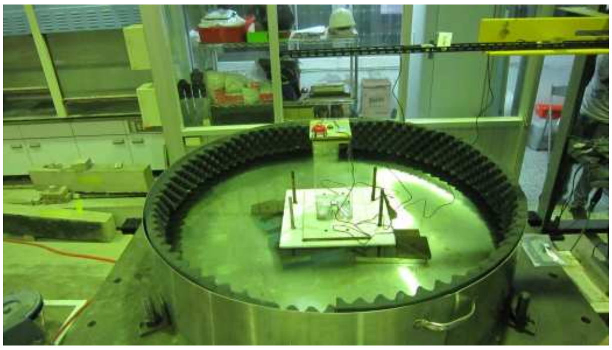

Figure 2.9. Arrangement of Tested model (DL type)

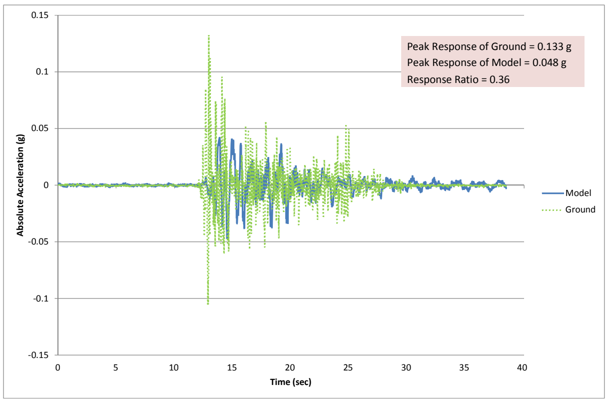

Figure 2.10. Comparison of The Acceleration Responses Between The Roof and The Ground Under The ew EL CENTRO Earthquake (NDL type)

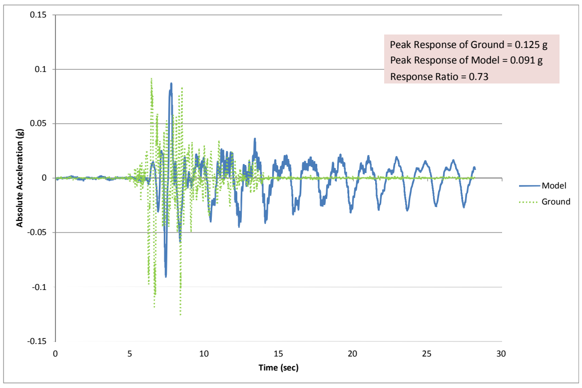

Figure 2.11. Comparison of The Acceleration Responses Between The Roof and The Ground Under The ew KOBE Earthquake (NDL type)

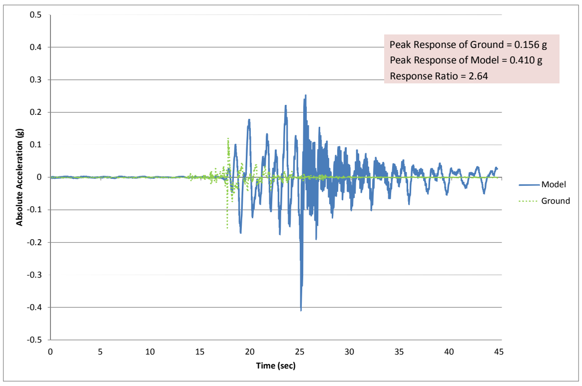

Figure 2.12. Comparison of The Acceleration Responses Between The Roof and The Ground Under The ew Chi-Chi Earthquake (NDL type)

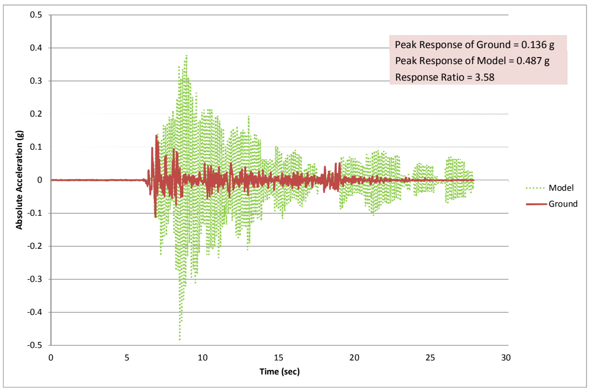

Figure 2.13. Comparison of The Acceleration Responses Between The Roof and The Ground UnderTthe ew EL CENTRO Earthquake (CC type)

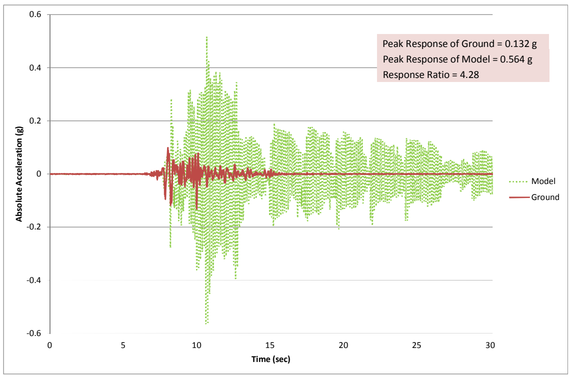

Figure 2.14. Comparison of The Acceleration Responses Between The Roof and The Ground Under The ew KOBE Earthquake (CC type)

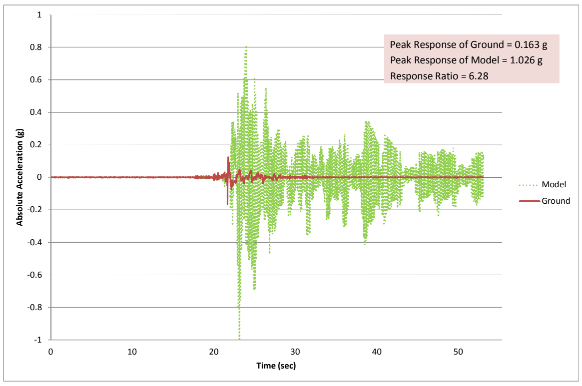

Figure 2.15. Comparison of the Acceleration Responses Between the Roof and the Ground Under the ew Chi-Chi Earthquake (CC type)

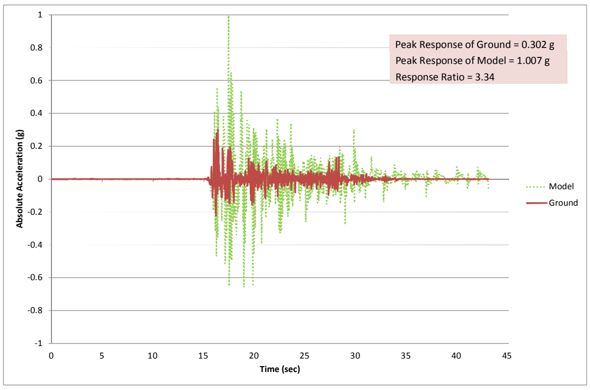

Figure 2.16. Comparison of the Acceleration Responses Between the Roof and the Ground Under the ew EL CENTRO Earthquake (DL1 type)

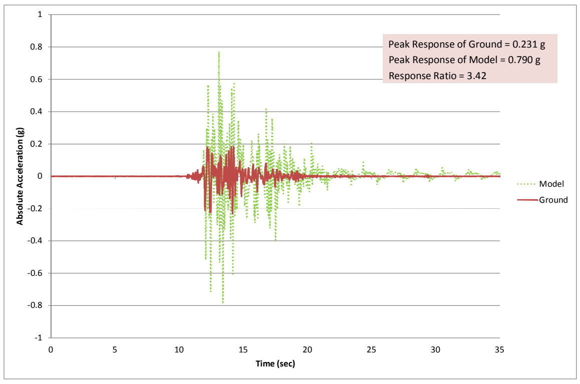

Figure 2.17. Comparison of the Acceleration Responses Between the Roof and the Ground Under the ew KOBE Earthquake (DL1 type)

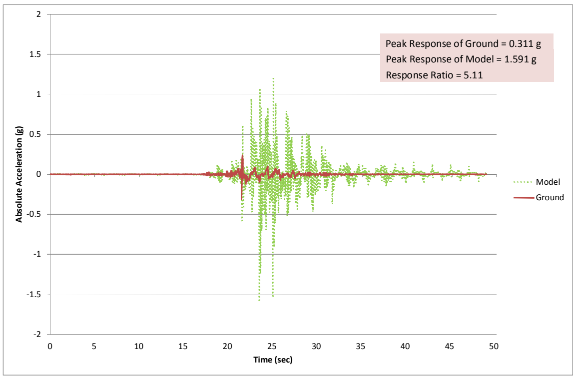

Figure 2.18. Comparison of the Acceleration Responses Between the Roof and the Ground Under the ew Chi-Chi Earthquake (DL1 type)

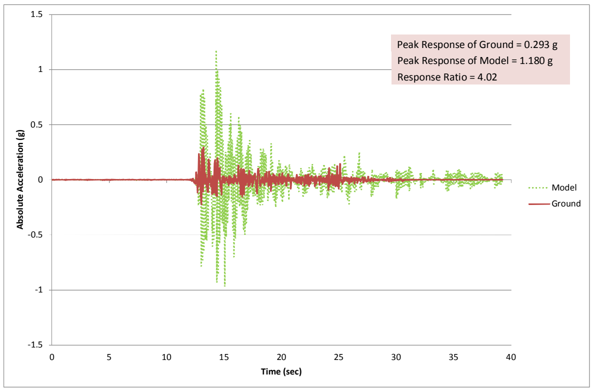

Figure 2.19. Comparison of the Acceleration Responses Between the Roof and the Ground Under the ew EL CENTRO Earthquake (DL2 type)

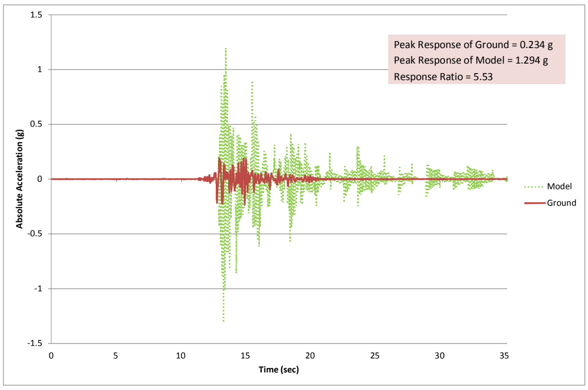

Figure 2.20. Comparison of the Acceleration Responses Between the Roof and the Ground Under the ew kobe Earthquake (DL2 type)

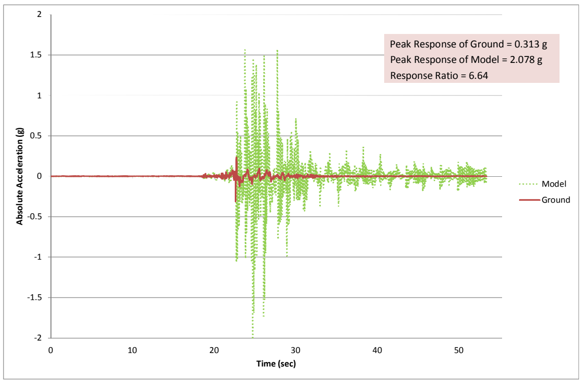

Figure 2.21. Comparison of the Acceleration Responses Between the Roof and the Ground Under the ew CHI-CHI Earthquake (DL2 type)

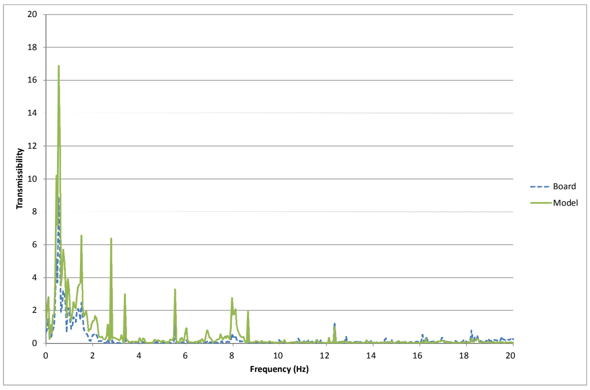

Figure 2.22. Transmmisibilities of Accelerations at Roof and the Floating Board Under the ew el CENTRO Earthquake (NDL type)

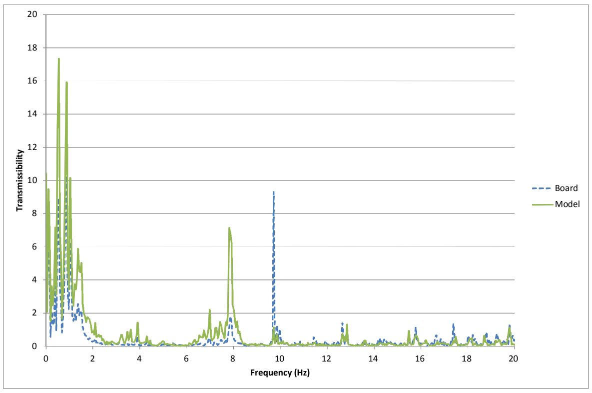

Figure 2.23. Transmmisibilities of Accelerations at Roof and the Floating Board Under the ew KOBE Earthquake (NDL type)

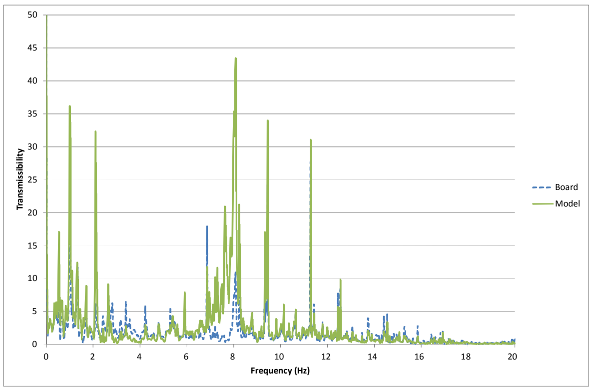

Figure 2.24. Transmmisibilities of Accelerations at Roof and the Floating Board Under the ew CHI-CHI Earthquake (NDL type)

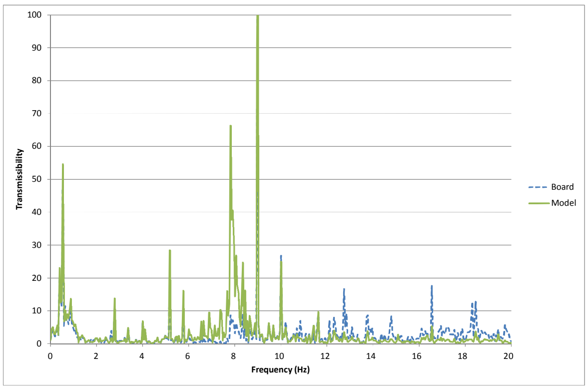

Figure 2.25. Transmmisibilities of Accelerations at Roof and the Floating Board Under the ew el CENTRO Earthquake (CC type)

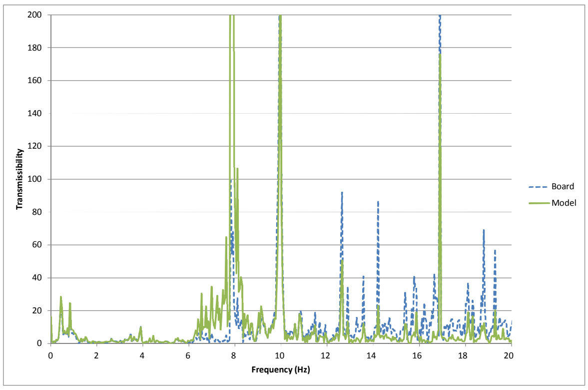

Figure 2.26. Transmmisibilities of Accelerations at Roof and the Floating Board Under the ew KOBE Earthquake (CC type)

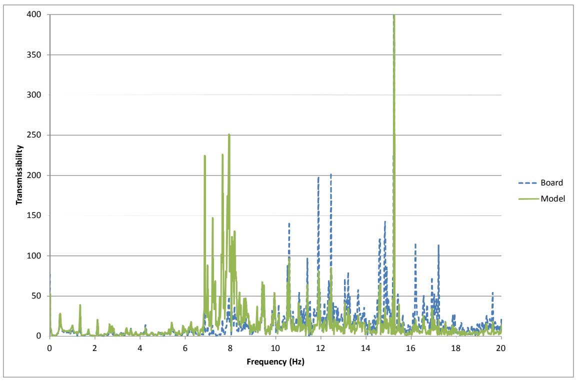

Figure 2.27. Transmmisibilities of Accelerations at Roof and the Floating Board Under the ew CHI-CHI Earthquake (CC type)

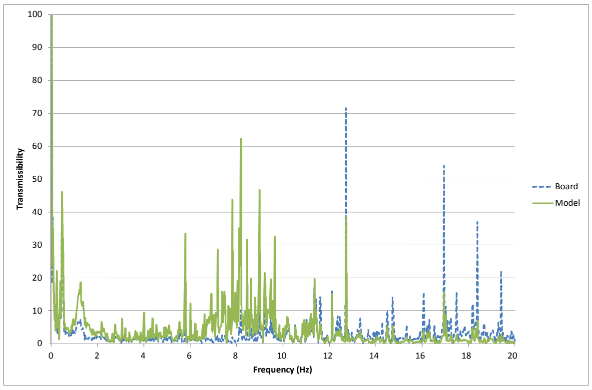

Figure 2.28. Transmmisibilities of Accelerations at Roof and the Floating Board Under the ew el CENTRO Earthquake (DL1 type)

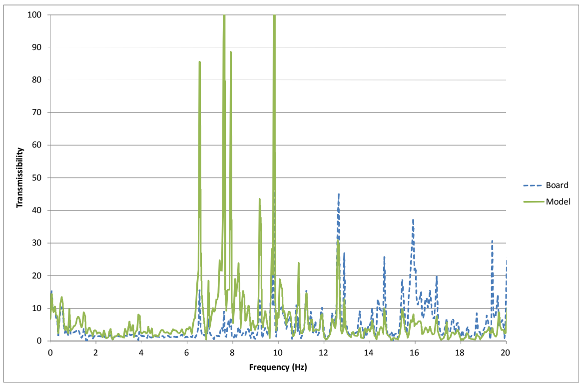

Figure 2.29. Transmmisibilities of Accelerations at Roof and the Floating Board Under the ew KOBE Earthquake (DL1 type)

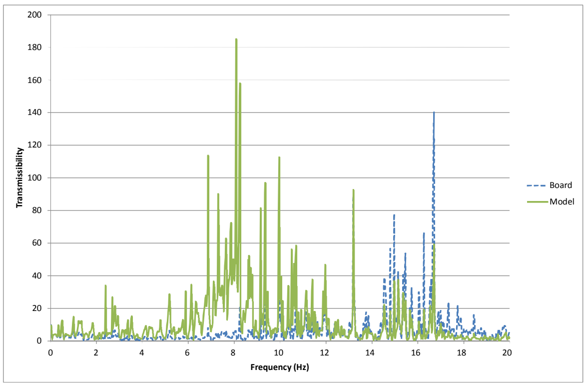

Figure 2.30. Transmmisibilities of Accelerations at Roof and the Floating Board Under the ew CHI-CHI Earthquake (DL1 type)

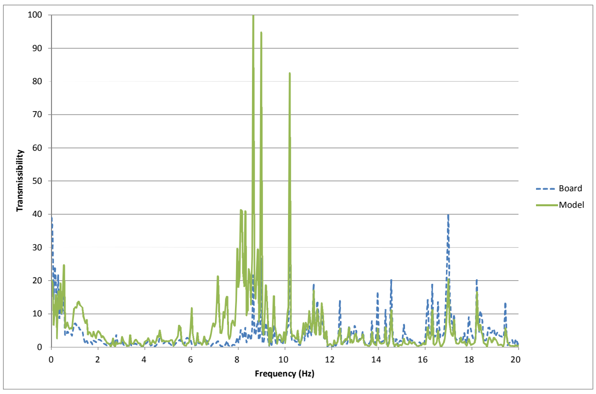

Figure 2.31. Transmmisibilities of Accelerations at Roof and the Floating Board Under the ew el CENTRO Earthquake (DL2 type)

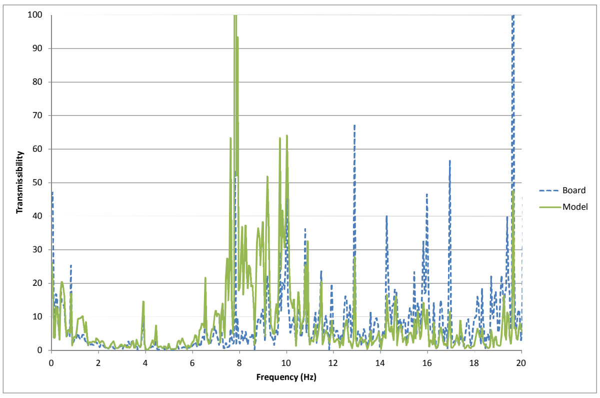

Figure 2.32. Transmmisibilities of Accelerations at Roof and the Floating Board Under the ew KOBE Earthquake (DL2 type)

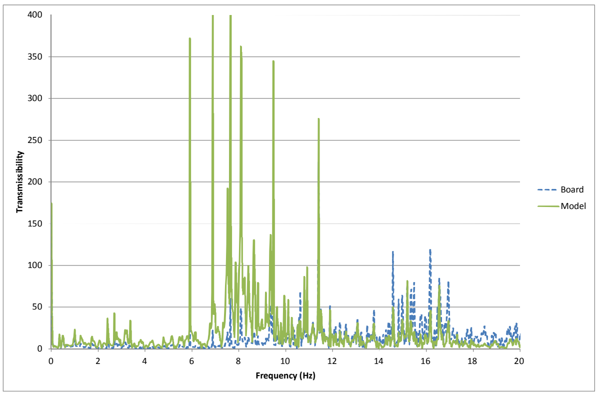

Figure 2.33. Transmmisibilities of Accelerations at Roof and the Floating Board Under the ew CHI-CHI Earthquake (DL2 type)